JOURNAL OF AGRICULTURAL AND FOOD CHEMISTRY

Effect of Gel Structure on the Dissolution of Heat-Induced β-Lactoglobulin Gels in Alkali

RUBEN MERCADÉ-PRIETO, ROBERT J. FALCONER, WILLIAM R. PATERSON, AND D. IAN WILSON*

Department of Chemical Engineering, University of Cambridge, Cambridge, Pembroke Street, CB2 3RA, United Kingdom

The dissolution of heat-induced β-lactoglobulin (βLg) gels in alkaline solution plays an important role in the cleaning-in-place of fouled dairy and other food plants. The dissolution behavior is strongly influenced by the conditions under which the gel is formed. At low alkaline pH values (<13), the dissolution rate constant k_g' decreases with longer gelation time and higher temperature. An inverse relationship is observed between the k_g' value and the amount of covalently cross-linked proteins in the gel, which is mainly due to disulfide bonds. β-Elimination kinetics of intramolecular cystines in βLg have been used to estimate the amount of intermolecular disulfide bonds that are cleaved during dissolution. The results call into question current dissolution models for these systems based on external mass transfer through the fluid next to the swollen gel. At low temperatures, the amount of disulfide cleavage is estimated to be small, indicating that dissolution is likely to involve the (slow) disengagement of large protein clusters, analogous to the dissolution of synthetic polymers.

KEYWORDS: Cleaning; β-elimination disulfide bonds; dissolution; β-lactoglobulin

INTRODUCTION

Protein gelation has been extensively studied in recent decades (*1*). One of the more extensively studied systems is the heat-induced gelation of whey proteins found in milk (*2*), especially β-lactoglobulin (βLg) (*3, 4*). Significant progress has been made in understanding the interactions involved during gelation (*5, 6*) and in particular the key role of thiol−disulfide exchange reactions (*7*−*9*). One area involving protein gels that has not received much detailed attention is in the cleaning of food-processing equipment, particularly in the dairy sector. Pasteurization and sterilization are primarily achieved by heat treatment, which results in the formation of fouling deposits on heat transfer and other surfaces. The deposits contain proteins, fats, sugars, and mineral salts (*10*). The removal of such deposits is critical to the dairy industry in terms of down time, energy, cleaning, hygiene, and waste treatment costs. Cleaning is usually performed by circulating alkaline solutions through the equipment in cleaning-in-place (CIP) operations. Proteins, and particularly βLg, constitute the bulk of milk-fouling deposits at low-temperature operations, and several models for cleaning have been proposed (*11*), but the mechanism is still not well-understood due to the complexity of the problem. For example, the effect of different protein interactions on the dissolution process has not been studied and which, if any, is most significant has not been determined. In this work, we study thermally induced whey protein gels, which have been used previously as a model for proteinaceous milk-fouling deposits (*12*). The dissolution conditions studied reflect those used in dairy CIP processes (pH > 12). Further understanding of the dissolution mechanism is likely to be relevant in the development of new applications of whey gels in the food or pharmaceutical sectors, for example, as drug carriers (*13, 14*).

Experimental studies of whey protein cleaning frequently report three stages, namely, an initial swelling stage, a "plateau" stage where the measured clearing rate (rate of change of protein concentration in solution) is relatively constant (R_o), and a final decay phase where this rate decreases to zero and all deposit is removed. Most of the removal occurs during the plateau stage, and this has been modeled as being controlled completely by external mass transfer, i.e., by diffusion and convection of the disengaged proteins through the film at the gel/fluid interface (*15*). Other steps, i.e., diffusion of hydroxyl groups from the NaOH solution into the gel, chemical reactions within the gel, and protein disengagement, were considered to be fast. More recently, Mercadé-Prieto and Chen (*16*) have demonstrated that the gelation conditions, such as gelation pH or temperature, have a significant influence on R_o. Such findings indicate that a mass transfer model is not a sufficient description of the mechanisms controlling dissolution. The aim of this study is to determine the influence of the gel structure on the dissolution rate of βLg heat-induced gels, by manipulating the gelling conditions, and to develop a more accurate mechanistic model. The interactions between the proteins in the gel will be determined by solubility measurements in different buffers. As disulfide bridges are known to be a key element of the gel network (*4, 8*), the

* To whom correspondence should be addressed. Tel: +44 1223 334791. Fax: +44 1223 334796. E-mail: diw11@cam.ac.uk.

10.1021/jf0605650 CCC: $33.50
Published on Web 07/04/2006

cleavage kinetics in alkali are determined in order to assess their relevance in the dissolution process.

EXPERIMENTAL PROCEDURES

Materials. βLg was kindly donated by Davisco Foods International, Inc. (Lesueur, MN). The composition of the powder as given by the manufacturer (lot JE 003-3-922) was 5.8% moisture, solids (d.b.), 97.4% protein of which 95.0% was βLg, 0.1% fats, and 2.4% ash. βLg powder and solutions prepared with deionized water were stored at 4 °C in airtight containers. The pH of the protein solutions was 7.45 ± 0.05. Reagents used were of analytical grade (Sigma, Fisher) and were used as received.

Methods. *Gel Formation.* Gels were formed inside cylindrical glass capsules, 10.8 mm i.d. and 40 mm high, using well-homogenized 8×10^{-3} M (~15 wt %) βLg solutions. The capsules were filled, closed with a plastic stopper, sealed with foil, and held in a water bath at the desired gelation temperature, T_{gel} (±0.1 °C), and gelling time, t_{gel}. The top 2 mm of the gel was removed with a spatula to ensure an even surface. Gels were kept at 4 °C overnight before use.

Dissolution. Dissolution tests were performed in batch mode, and the dissolution rate was calculated by measuring the increase in the concentration of protein in the alkali solution over time (*16*). In brief, 250−1000 mL of the solvent was added to a glass bottle held in a water bath (±0.3 °C) and agitated using a magnetic stirrer. The solution pH was verified by titration (0.1 N HCl standard, Riedel-de Haën). A small fraction of the solution was recirculated through a UV spectrometer (Unicam 8625) using a peristaltic pump. The absorbance of the dissolved protein was continuously recorded at 20 s interval with a LabView (National Instruments) application for at least 8000 s. Three wavelengths were recorded simultaneously for better accuracy: 204, 214, and 224 nm for deionized water and 224, 250, and 280 nm for alkaline solutions. Extinction coefficients were established for each pH condition. Dissolution rates were calculated using numerical three-point differences of the mean concentration and finally smoothed by a moving average in order to remove the noise. Mechanical erosion of gels inside capsules when using low stirring speeds (~350 rpm) has been shown to be negligible (*16*).

Solubilization. Samples were solubilized in three different solutions as reported in the literature (*17*, *18*), namely, (i) pH 8 buffer (0.086 M Tris, 0.09 M glycine, and 0.004 M EDTA); (ii) buffer i plus denaturants [6 M urea and 0.0173 M sodium dodecyl sulfate (SDS)]; and (iii) buffer ii plus 0.01 M dithiothreitol (DTT). About 0.02−0.06 g of gel was introduced into 25 mL centrifuge tubes with 20 mL of solubilizing solution. The protein solution was homogenized at room temperature using an Ultra-Turrax T18 homogenizer for 60 s at 24000 rpm (buffer i) or 15 s at 24000 rpm plus 45 s at 18000 rpm (buffers with denaturants) followed by 30 min of centrifugation at 19500 rpm below 10 °C. The protein concentration in the supernatant was measured via its absorbance at 280 nm (UV1, Thermo Spectronic). A blank solution without any gel and a blank solution with 0.25 g L^{-1} βLg were used as controls. The supernatant of some gels solubilized with a 0.02 M DTT buffer solution was analyzed with SDS−polyacrylamide gel electrophoresis (PAGE) (NuPage 4−12% Bis-Tris Gel, Invitrogen), following the standard procedure for the precast gels under reducing conditions, MES buffer, and SimplyBlue SafeStain (Invitrogen) as detailed by the manufacturer. The protein loading in these SDS−PAGE tests was 6 μg per well.

β-Elimination Kinetics. The kinetics of the β-elimination of intramolecular disulfide bonds of βLg in solution were determined by independently checking the formation of persulfides (*19*) and dehydroalanine (*20*). The kinetic parameters obtained at room temperature agreed within experimental accuracy regardless of the method used. Persulfide formation was determined at 335 nm at room temperature (22 ± 1 °C) for different βLg and NaOH concentrations. The temperature dependency of the reaction was determined by following the formation of dehydroalanine (*20*), as it is more stable than persulfides at high temperatures (*21*). Dehydroalanine formation was checked at 241 nm using the dissolution apparatus with solutions of 2.35×10^{-5} M βLg and 0.063 M NaOH at various temperatures.

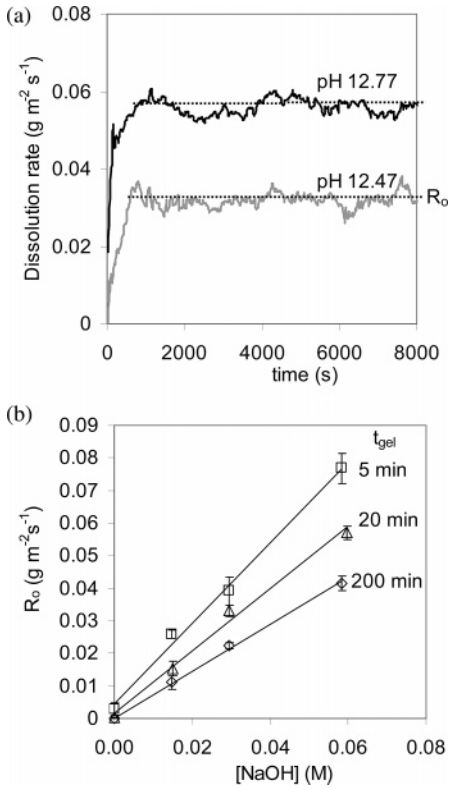

Figure 1. Dissolution rate of heat-induced gels at 24 °C and relatively low alkaline pH. (**a**) Rate profiles at different dissolution pH values. Gelation conditions: 8 mM βLg, pH 7.45, 80 °C for 20 min. (**b**) Constant dissolution rate R_o at different NaOH concentrations for gels formed at 80 °C and different t_{gel} values. Error bars show the standard deviation of the mean rate value. Lines show regression of data to eq 1 with best fit k_g'.

NaOH Penetration Depth. The depth of NaOH penetration into the gels was monitored by taking pictures of the swollen layer at different times, for up to 10 h, in duplicate experiments. The demarcation of the swollen layer was enhanced by adding four drops of phenolphthaleine to the protein solution before gelation (*22*).

RESULTS AND DISCUSSION

Dissolution Rate of β-Lactoglobulin Gels. The dissolution rate profile of βLg heat-induced gels was found to resemble those reported for whey protein concentrate (WPC) gels (*16*) for semi-infinite dissolution experiments. At "low" alkaline pH (12−13), **Figure 1a** shows that the dissolution rate increases during the initial swelling stage to a constant value with time, R_o, in the plateau stage (*23*). **Figure 1b** shows that the R_o data can be modeled successfully as

$$R_o = \frac{1}{A}\left(\frac{dn}{dt}\right)_{plateau} = k_g'[OH^-] + R_w \qquad (1)$$

where R_w denotes the dissolution rate in water (pH 7) (*16*), A is the exposed gel−solution interface area, here 9.2×10^{-5} m^2, n is the amount of protein dissolved, k_g' is the pseudo-kinetic constant, and [OH^-] is the hydroxide concentration in the bulk solution. Strictly speaking, these "dissolution rates" are fluxes but we use the terminology common to the literature.

The dissolution rate profiles observed at higher alkaline pH (>13) such as **Figure 2** are noticeably different: The dissolution rate is smaller at higher pH and decreases over time. Similar differences were reported previously for WPC gels (*16*). The dissolution rate therefore exhibits a maximum at an optimal sodium hydroxide concentration, which is a well-established

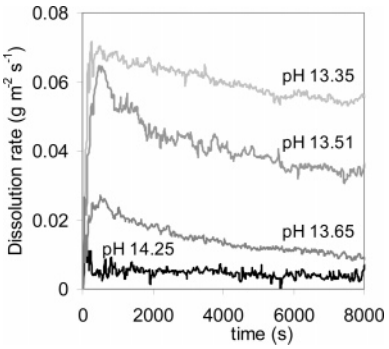

Figure 2. Dissolution rate profile at high pH, showing a decrease in rate with increasing pH. Gelation conditions are as in **Figure 1a**.

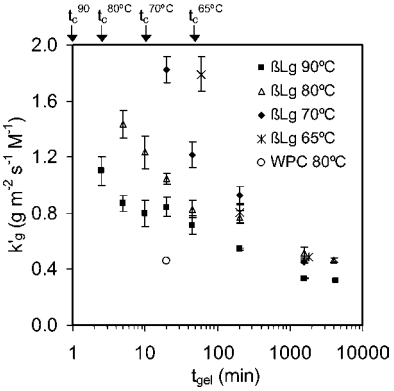

Figure 3. Dissolution rate constant k_g' for heat-induced gels formed at different t_{gel} and T_{gel} values. k_g' values are calculated as shown in **Figure 1b**; error bars show the standard deviation of the fitted parameter. The value reported for WPC gels is that reported by Mercadé-Prieto and Chen (*16*). The critical gelation times t_c for each T_{gel} are marked with arrows. Gelation conditions: 8 mM βLg and pH 7.45.

phenomenon in cleaning experiments (*24*). The dissolution of βLg gels has shown the same behavior observed in WPC gels; therefore, βLg can be used successfully as a model whey protein.

Effect of Gelation Conditions on Dissolution Rate. In this work, the effects of two gelation parameters are studied in detail: gelation time (t_{gel}) and gelation temperature (T_{gel}). **Figure 1b** shows that at low alkaline pH values (<13), R_o is smaller for gels formed at longer t_{gel}, but the first-order dependency on [OH$^-$] in eq 1 is maintained. Similar behavior is observed for gels formed at different T_{gel} values (65−90 °C). Both k_g' and R_w are affected by the gelation conditions: **Figure 3** shows how k_g' greatly decreases when overcuring the gels (t_{gel} longer than the critical gelation time, t_c). The t_c for the βLg used has been determined as detailed in Mercadé-Prieto and Chen (*22*) and was found to be ∼1 min at 90 °C, 2.6 min at 80 °C, 10.8 min at 70 °C, and 50 min at 65 °C. The k_g' value reported for 16.7 wt % WPC heat-induced gels in **Figure 3** is significantly lower than that for βLg gels formed under the same conditions. Future work will be performed to elucidate the source of this difference (e.g., the presence of other proteins, such as bovine serum albumin (BSA) and α-lactalbumin, and higher salt concentration).

The sensitivity of the dissolution rate at low alkaline pH to gelation conditions is not observed at higher pH values. **Figure 4a** shows dissolution rate profiles for gels prepared at different t_{gel} and dissolved at pH 13.65. The initial peak rate, R_{peak}, is larger for gels made at lower t_{gel} and T_{gel}; however, the final rate values, R_{end}, are similar (**Figure 4b**). Average values of 0.010 ± 0.002 g m^{-2} s^{-1} for gels formed at 80 °C and 0.008 ± 0.001 g m^{-2} s^{-1} for 90 °C gels appear to describe R_{end} well

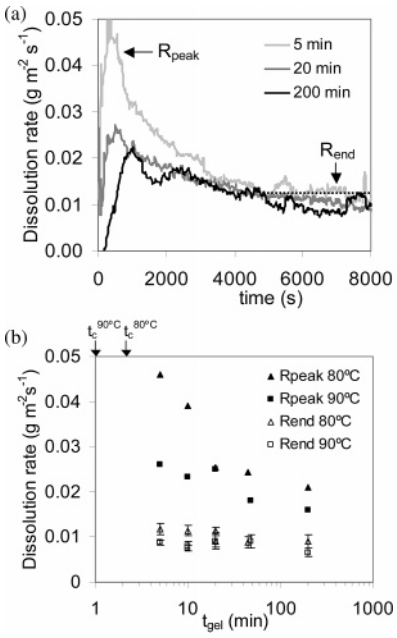

Figure 4. Effect of gelation conditions on the dissolution rate at pH 13.65 and 24 °C. (**a**) Rate profile with time for gels made at 80 °C and different t_{gel} values. (**b**) Effect of t_{gel} and T_{gel} values on the initial high rate (R_{peak}) and final rate (R_{end}). R_{end} is calculated as the mean over the last 3000 s, as shown by the construction in panel **a**.

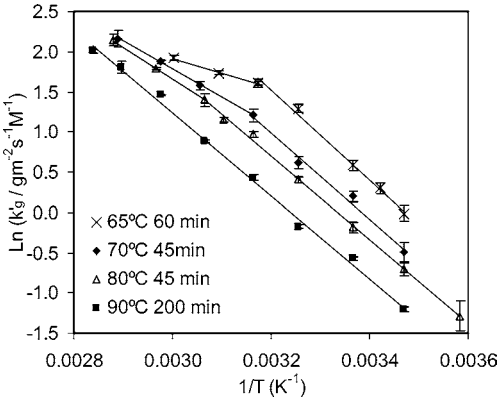

Figure 5. Arrhenius plot of the dissolution rate constant k_g' for gels formed at four different gelling conditions. Lines show the constructions for the best-fitted activation energies, summarized in **Table 1**.

across the t_{gel} range. Considering the major impact of t_{gel} and T_{gel} on k_g' (**Figure 3**), these are minor differences.

Effect of Dissolution Temperature. k_g' was measured for four types of gels across a wide range of temperatures, and the results are presented as a pseudo-Arrhenius plot in **Figure 5**. At lower temperatures, the temperature dependence in k_g' is independent of gelation conditions, with an average activation energy, E_a, of 44 kJ mol^{-1} (**Table 1**). At higher temperatures, however, a lower value of E_a, between 15 and 33 kJ mol^{-1} (**Table 1**), is observed for gels with high k_g' values. This decrease is most likely due to mass transfer limitations, either of diffusion of NaOH into the gel or of protein away from the surface.

Solubility of Gels. Total solubility measurements are a convenient way to estimate the proportion of the different protein interactions in gels or films (*17*, *18*, *25*). Proteins dissolved in the pH 8 buffer (Tris-Gly-EDTA) correspond to those stabilized by electrostatic interactions or hydrogen bonds, as well as unbounded proteins. This buffer plus denaturants (urea−SDS)

Table 1. k_g' Activation Energies for Gels Prepared under Four Different Gelling Conditions

gelation conditions	dissolution T range (°C)	E_a (kJ mol^{-1})
65°C, 60 min	15–42	46 ± 2
	42–60	15 ± 2
70°C, 45 min	15–43	44 ± 3
	43–73	29 ± 1
80°C, 45 min	6–53	43.5 ± 1
	53–74	33 ± 2
90°C, 200 min	15–79	43 ± 1

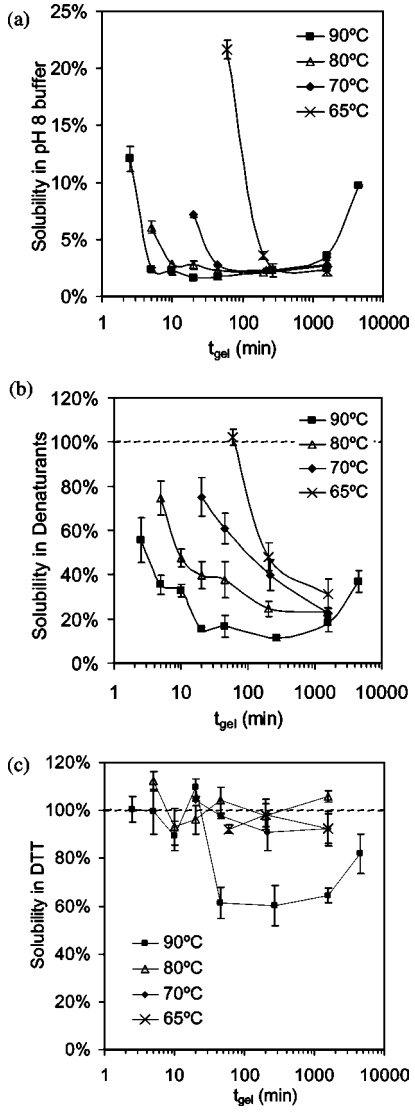

Figure 6. Total solubility of βLg gels formed at different t_{gel} and T_{gel} values in different buffers: (**a**) Tris-Gly-EDTA, pH 8 buffer; (**b**) pH 8 buffer plus denaturants (6 M urea and 0.0173 M SDS); and (**c**) pH 8 buffer with denaturants plus 0.01 M DTT. Error bars show the standard deviation of triplicate experiments.

can disrupt the previous interactions as well as hydrophobic ones. Finally, the buffer with denaturants and DTT can also reduce disulfide bonds.

Figure 6a shows that the solubility of βLg gels in the pH 8 buffer is very small, at 2−3%. Only those gels formed close to t_c exhibit a significantly higher solubility. **Figure 6b** shows that the gels are much more soluble in the presence of denaturants, but the solubility is greatly reduced at longer t_{gel} and higher T_{gel}. The proteins that remain insoluble in the presence of

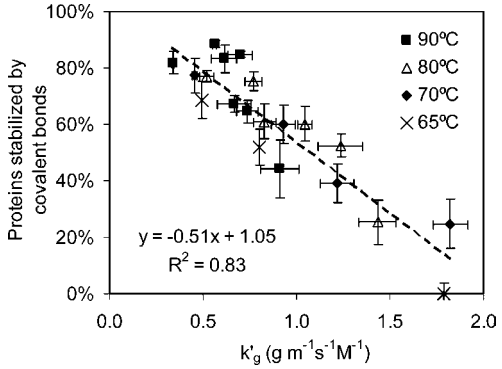

Figure 7. Correlation between the percentage of proteins stabilized by intermolecular covalent bonds (the insoluble part in **Figure 6b**) and the rate constant k_g' for gels formed at different t_{gel} and T_{gel} values (from **Figure 3**). The dashed line shows the best fit through all data.

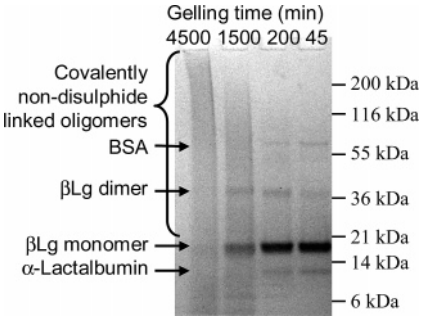

Figure 8. Reducing SDS–PAGE of the supernatant of gels formed at 90 °C at different t_{gel} values, solubilized in a standard buffer with denaturants and 0.02 M DTT.

denaturants correspond to covalently cross-linked protein clusters (*25*). DTT can break down these clusters increasing the gel solubility to 100% as shown in **Figure 6c**; the gels that are only partially soluble in DTT are discussed subsequently. The similarity between the separate plots of solubility in denaturants (**Figure 6b**) and k_g' (**Figure 3**) against t_{gel} and T_{gel} is remarkable. **Figure 7** illustrates the good agreement between the amount of proteins stabilized by intermolecular covalent bonds, estimated as the insoluble part in the buffer with denaturants (*25*), and the dissolution rate constant k_g'. More intermolecular cross-links in the gel network make the dissolution process slower. Therefore, the gel structure, in particular the amount of covalent cross-links, ought to be included in the dissolution mechanism, and this is not the case for external mass transfer controlled dissolution models.

The origin of these covalent cross-links is the thiol−disulfide exchange reactions during gelation. The importance of intermolecular disulfide bonds in the formation and structure of βLg heat-induced gels has been reported at length (*8*, *18*). Their importance in solubilization is demonstrated in **Figure 6c**: The gels are completely soluble in DTT, which is known to cleave disulfide bonds, whereas buffers in **Figure 6a**,**b** are not expected to affect disulfide bonds. Therefore, k_g' is inversely related to the amount of intermolecular disulfide bonds.

Nondisulfide Covalent Cross-Links. The gels formed at 90 °C and t_{gel} > 45 min are not completely soluble in DTT (60−80% gel solubility, **Figure 6c**). This feature was investigated using reducing SDS−PAGE of gels solubilized in DTT to establish whether covalent cross-links other than intermolecular disulfide bonds give rise to the decrease in solubility. In **Figure 8**, the gel formed at 90 °C and 45 min shows an intense band for the βLg monomer, with bands for α-lactalbumin and BSA

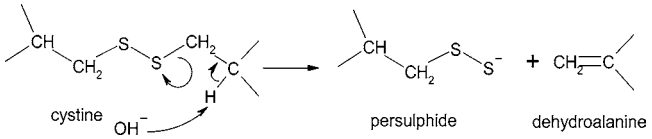

Figure 9. β-Elimination mechanism of disulfide bonds in alkali (*31*).

impurities. There is also a faint band for the βLg dimer, whose intensity grows with longer t_{gel}. Beyond 1500 min, continuous bands below monomeric βLg imply that the proteins are being hydrolyzed. In addition, the bands above the βLg monomer suggest that partly hydrolyzed oligomers are formed through nondisulfide covalent cross-links. These bonds are most probably formed by the nucleophilic addition to dehydroalanine of other amino acids such as lysine, forming lysinoalanine (LAL) (*26*). This nonnatural amino acid has long been observed in milk proteins treated at high temperatures (*27*). Even though it has been reported that small aggregates can be formed through interprotein LAL formation (*28*, *29*), it is not known that LAL could be involved in the structure of a protein gel. Following this hypothesis, the gel formed at 90 °C for 4500 min is remarkable. **Figure 8** shows that the proteins are so damaged that even the βLg monomer band is no longer visible. In consequence, the solubility in all three buffers increases as compared to gels made at shorter t_{gel} values (**Figure 6**). However, this is not translated into a larger dissolution rate constant k_g'; in fact, it is the smallest measured (**Figure 3**). This may be explained because only high temperatures (>60 °C) have been reported for the alkali cleavage of LAL (*30*). At room temperature, the NaOH may not be able to destroy those bonds.

***β*-Elimination of Disulfide Bonds.** Disulfide bonds have been shown to be the main interaction in the gels that restricts the dissolution process. Therefore, it is of interest to know the kinetics of its cleavage by NaOH in order to be able to estimate the proportion of disulfide bonds that is reduced when the proteins are dissolved. The alkali cleavage mechanism of disulfide bonds in proteins has been reported to follow a β-elimination mechanism (*31*) as shown in **Figure 9**. Gawron and Odstrchel (*21*) proposed the following kinetic model to describe the β-elimination of several cystine derivates:

$$r = k_{\beta E}[OH^-][RS_2R] = k_{\beta E}'[RS_2R] \qquad (2)$$

where r is the reaction rate, $k_{\beta E}$ is the β-elimination kinetic constant, $[RS_2R]$ is the concentration of disulfide, and $k_{\beta E}'$ is the pseudo-kinetic constant defined as $k_{\beta E}' \equiv k_{\beta E}[OH^-]$. Although eq 2 has been found to be valid for several proteins (*19*), βLg has not been studied in detail (*32*). By following the formation of persulfides at 335 nm (*33*), the first-order dependency on the disulfide concentration (data not shown) and on the hydroxide concentration (**Figure 10**) was confirmed. The kinetic parameters obtained are of the same order of magnitude as those reported for other proteins, as shown for ribonuclease A (see **Figure 10**) (*34*). The temperature dependency of $k_{\beta E}$ was determined by following the formation of dehydroalanine at 241 nm (*20*) (**Figure 11**). Predenaturation by leaving βLg in 8 M urea overnight did not enhance the β-elimination rate, nor change its temperature dependence (**Figure 11**), as has been reported for lyzozyme (*20*). This suggests that alkali alone is sufficient for denaturing βLg and exposing the disulfide bonds to the solvent. The $k_{\beta E}$ activation energy obtained, 76.4 ± 0.9 kJ mol^{-1}, compares favorably with the range of 60−100 kJ mol^{-1} reported previously for several proteins and particularly the 83 kJ mol^{-1} reported for BSA (*20*). The preexponential factor $k_{\beta E}$ was 3.5×10^{12} M^{-1} min^{-1}.

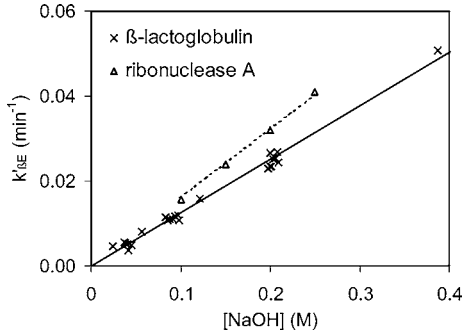

Figure 10. Effect of NaOH concentration on the pseudo-first-order β-elimination kinetic constant $k_{\beta E}'$, calculated by monitoring persulfide formation at 335 nm and 22 °C. Lines show the best fit $k_{\beta E}$ value (eq 2), 0.126 ± 0.016 M^{-1} min^{-1} for βLg. Data for ribonuclease A at 25 °C were taken from Florence (*34*).

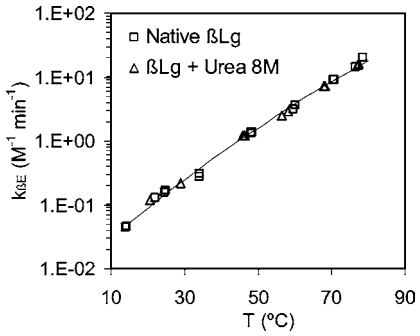

Figure 11. Effect of the temperature on the β-elimination constant $k_{\beta E}$ for untreated βLg and βLg denatured overnight in 8 M urea. $k_{\beta E}$ away from room temperature is calculated by measuring the dehydroalanine formation at 241 nm. The line shows the best fit regression model for E_a, 76.4 kJ mol^{-1}.

DISCUSSION

Several of the mechanisms proposed to date to model the cleaning of milk-related fouling deposits using alkaline solutions are based on the assumption that the limiting elementary process is the diffusion of the solubilized products through the boundary layer (*11*, *35*). Analogous models exist for the dissolution of polymers (*36*). However, the profound effect of gelation conditions on R_o is difficult to reconcile with a mechanism controlled solely by the external mass transfer (*11*, *35*). In this work, we have shown how greatly the gelation conditions modify k_g' for gels formed with the same protein concentration (**Figure 3**), only by changing the degree of cross-linking. **Figure 7** show that k_g' is inversely related to the amount of covalent cross-linking in the gel structure, which is essentially due to disulfide bridges. The β-elimination mechanism has been shown to be involved in the alkali cleavage of intramolecular disulfide bonds, and there is no ground to doubt that another mechanism is responsible for the reduction of intermolecular disulfide bridges. This evidence may support the hypothesis that chemical reactions, and in particular β-elimination, may be the limiting mechanism in dissolution (*16*). However, a mechanism where the dissolution process is wholly controlled by the rate of formation of "removable" aggregates via chemical reaction is not completely plausible. In such a model, the dissolution rate should be directly related to the cleavage reaction rate; therefore, the dissolution rate should exhibit similar temperature dependence to the chemical reaction. The E_a values in **Table 1** for k_g' at low dissolution temperatures, which was insensitive to the gelation conditions (**Table 1**), are noticeably smaller than that for the β-elimination reaction, at 44 and 76 kJ mol^{-1},

Table 2. Parameters of the Hydroxide Penetration Model[a]

[OH] (M)	δ_{OH}[b] (mm)	R_0[c] (g m^{-2} s^{-1})	ν_{LG}[d] (μm s^{-1})	$\Delta t_{\delta OH}$[d] (min)	[SS]/[SS]$_0$[d] (%)
0.0076	1.70 ± 0.17	0.0065	0.04	715	78
0.015	1.17 ± 0.11	0.013	0.08	252	84
0.023	0.71 ± 0.05	0.019	0.12	103	90
0.030	0.85 ± 0.09	0.025	0.15	93	88
0.045	0.81 ± 0.05	0.038	0.23	60	89
0.060	0.99 ± 0.07	0.050	0.30	54	86
0.074	0.99 ± 0.12	0.062	0.38	44	86

[a] Gelation conditions: heat-induced gels formed at 80 °C for 45 min and dissolved at 21°C. [b] Measured experimentally. [c] Calculated using eq 1. [d] Calculated as outlined in the Appendix.

Table 3. Hydroxide Penetration Model Parameters for Gels Made at Different Gelling Conditions and Different Dissolution Temperatures[a]

gelling conditions	T (°C)	δ_{OH}[b] (mm)	R_0[c] (g m^{-2} s^{-1})	ν_{LG}[d] (μm s^{-1})	$\Delta t_{\delta OH}$[d] (min)	[SS]/[SS]$_0$[d] (%)
80 °C, 45 min	38	0.82 ± 0.09	0.11	0.67	20	74
80 °C, 45 min	50	0.62 ± 0.09	0.20	1.2	8.5	70
80 °C, 45 min	60	0.55 ± 0.06	0.30	1.8	5.0	61
65 °C, 60 min	21	0.63 ± 0.06	0.087	0.57	20	95
70 °C, 45 min	21	0.75 ± 0.08	0.053	0.32	39	91

[a] Dissolution in 0.060 M NaOH. [b] Measured experimentally. [c] Calculated using eq 1. [d] Calculated as outlined in the Appendix.

respectively. In addition, we have found that the β-elimination reactions do not occur fast enough to support such a model, as explained subsequently.

The amount of nonreduced disulfide bonds, [SS]/[SS]$_0$, in the protein clusters near the gel−liquid interface, at the moment of removal, can be calculated as outlined in the Appendix. [SS]/[SS]$_0$ can be estimated from the constant NaOH penetration depth in the gel, δ_{OH}, the dissolution rate, and the β-elimination kinetics. **Table 2** reports these parameters for gels formed at 80 °C and 45 min and then dissolved at different NaOH concentrations at 21 °C. The calculated [SS]/[SS]$_0$ values are greater than 85% at most NaOH concentrations. Similar values are found at different gelation conditions when the gels are dissolved at 21 °C (**Table 3**). These high values imply that the protein clusters released from the semi-infinite gel network still contain most of the intermolecular disulfide bonds and thus have a size similar to that before dissolution. Only at high temperatures does the ratio [SS]/[SS]$_0$ decrease significantly (**Table 3**).

Most of the gels studied have solubilities below 50% in urea and SDS (**Figure 6b**). The amount of large clusters will decrease in a direct manner with [SS]/[SS]$_0$, at ∼15% at room temperature (**Table 2**). Therefore, at the moment of dissolution, a significant percentage of the proteins in the gel will still form part of a large cluster. These clusters, about 1.8×10^6 Da for the 100 monomer primary aggregates observed during the gelation process (*37*), are expected to be disengaged very slowly from the gel matrix. In the dissolution of polymers, diffusion control is predicted for low molecular weight polymers and disengagement control is predicted for large polymers (*38*, *39*). The small decrease of [SS]/[SS]$_0$ suggests that the second scenario is the most likely in βLg gels. In such a model, where the protein disengagement is slow, two key parameters would be the number and the size of the large clusters in the gel, which are both related to the cross-linking degree of the gel, and therefore also in agreement with **Figure 7**.

The strong sensitivity of the dissolution rate to the gelation conditions at lower pH is not observed when using a pH well above 13 (**Figure 4a**,**b**). Therefore, the low dissolution rates found in those conditions are unlikely to be related to the different initial gel structure, as has been discussed above for lower pH values. It has been suggested that at high pH, new cross-links may be formed in the gel structure, in analogy to caustic-induced gels made at high pH, explaining the small rate observed (*16*). This hypothesis requires that the gel structure is completely irreversibly modified during the treatment at high pH, which has been shown not to be the case (*40*). It was concluded that it was probably the effect of the solvent, rather than the final gel structure, which was involved in the low dissolution rates observed (*40*). Bird (*41*) proposed initially that the existence of an optimum cleaning concentration was related to the more open pore structure of the protein deposits as observed by scanning electron microscopy. Micrographs above this concentration (0.5 wt % NaOH, pH 13.1) suggested that the whey deposits swelled less. However, as swelling is related to the protein surface charge, it was not clear why such a swelling optimum should exist. Nevertheless, this swelling behavior has been recently reported in hydrogels with similar backbone structures to proteins (*42*). In those hydrogels, the maximum swelling ratio collapsed at pH 13−14 to a fifth its value at their optimum pH. It was proposed that at high pH, the screening effect of the counterions (Na^+) hinders, and eventually opposes, the swelling at high concentrations (*42*). Such explanation should also be valid for protein gels and would agree well for a dissolution mechanism where the disengagement of the protein clusters is a slow process. These hypotheses are the subject of ongoing work.

This work has concentrated on elucidating the fundamental reaction/dynamic steps involved in the dissolution of these whey protein gels. In practice, the gels are also subject to shear from the flow of the cleaning agent, which will affect mechanical and mass transport-related steps. However, the impact of shear can only be assessed once shear-free dissolution is understood.

In conclusion, βLg heat-induced gels have been successfully used as a model system to study the alkali dissolution of whey protein gels. Equation 1, which was developed on the basis of WPC studies, has proved to be applicable, although larger k_g' values have been found for βLg gels. We have confirmed that the gelation conditions, particularly T_{gel} and t_{gel}, have a profound effect in k_g'. The variation in rates observed in different gels dissolved at the same conditions is difficult to explain using external mass transfer models (*35*). We have observed an inverse relationship between the decrease of k_g' and the increase in covalently linked (mainly disulfide bonds) proteins in the gels. The estimated amount of disulfide bonds cleaved at the moment of dissolution is too small for a chemical reaction control only dissolution scheme, as proposed by Mercadé-Prieto and Chen (*16*). This observation suggests that β-elimination reactions break down the percolating gel matrix, but they do not occur fast enough to reduce the size of the large clusters formed. In these conditions, when high molecular size fragments ($>10^6$ Da) are to be released, polymer dissolution models (*38*) predict that the disengagement of these long chains will be the slowest step. On the other hand, at high dissolution pH (>13), the characteristically small rates observed are highly insensitive to the gelling conditions.

ACKNOWLEDGMENT

We are grateful to Davisco for providing the βLg.

APPENDIX

Figure 12 is a schematic representation of the NaOH diffusion into a gel to yield a swollen layer that dissolves. In

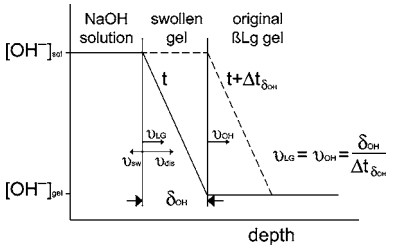

Figure 12. Schematic diagram of the NaOH concentration with depth in a gel when a constant NaOH penetration depth δ_{OH} is observed.

Fickian diffusion analyses of such a system, the linear velocity of NaOH penetration, v_{OH}, is inversely proportional to the penetration depth, δ_{OH}. As the velocity of the gel−liquid interface, v_{LG}, is independent of δ_{OH}, both velocities reach the same value after a certain time, after which δ_{OH} is constant. As the βLg gels dissolve quite quickly in comparison to WPC gels (*16*), a constant δ_{OH} is usually seen in less than 1 h. v_{LG} is comprised of the dissolution contribution, v_{dis}, minus the swelling velocity of the gel where the NaOH has penetrated, v_{sw}: v_{dis} is related to R_o by

$$v_{LG} = v_{dis} - v_{sw} = \frac{R_o}{\rho_{sw} C_{\beta Lg,sw}} - v_{sw} \qquad \text{(A1)}$$

As v_{sw}, the density, ρ_{sw}, and the mass concentration of βLg in the swollen layer, $C_{\beta Lg,sw}$, are all unknown, it is a fair approximation to suggest that v_{LG} is independent of swelling. The increase of v_{dis} due to a lower $C_{\beta Lg,sw}$ caused by the swelling will be compensated by the presence of a v_{sw} term. Therefore,

$$v_{LG} \approx \frac{R_o}{\rho_{gel} C_{\beta Lg,gel}} \qquad \text{(A2)}$$

where the density and the mass concentration of βLg are now those for the original gel, at about 1.1 g mL^{-1} (*35*) and 0.15 g βLg g gel^{-1} respectively. Finally, the time that a slice of gel is in contact with the NaOH before it is dissolved is

$$\Delta t_{\delta OH} = \frac{\delta_{OH}}{v_{LG}} \qquad \text{(A3)}$$

Solving the kinetic eq 2 for a fixed position of the gel over time $\Delta t_{\delta OH}$ yields the ratio of disulfide bonds that have not been β-eliminated, [SS]/[SS]$_0$, eq A4:

$$\frac{[SS]}{[SS]_0} = \exp([OH^-]_{Av,\delta OH} k_\beta E \Delta t_{\delta OH}) \cong \exp(0.463\,[OH^-]_{sol} k_{\beta E} \Delta t_{\delta OH}) \qquad \text{(A4)}$$

where $[OH^-]_{Av,\delta OH}$ is the average hydroxide concentration in the swollen layer. Assuming a linear profile of hydroxide concentration with depth, $[OH^-]_{Av,\delta OH}$ is half the concentration in the solution, $[OH^-]_{sol}$, although a detailed Fickian simulation shows that it is closer to $0.463 \times [OH^-]_{sol}$. We assume that $k_{\beta E}$ and its activation energy for intermolecular disulfide bonds are similar to that calculated for intramolecular cystines. Therefore, eq A4 also represents the amount of intermolecular disulfide bonds that have not been cleaved in a $\Delta t_{\delta OH}$ interval.

LITERATURE CITED

(1) Clark, A. H. Gelation of globular proteins. In *Functional Properties of Food Macromolecules*, 2nd ed.; Hill, S. E., Ledward, D. A., Mitchell, J. R., Eds.; Aspen Publishers: Gaitherburg, MD, 1998; pp 77−142.

(2) Aguilera, J. M. *Food Technol.* **1995**, 83−89.

(3) Lefèvre, T.; Subirade, M. *Biopolymers* **2000**, *54*, 578−586.

(4) Hoffmann, M. A. M.; Van Mil, P. J. J. M. *J. Agric. Food Chem.* **1999**, *47*, 1898−1905.

(5) Havea, P.; Carr, A. J.; Creamer, L. K. *J. Dairy Res.* **2004**, *71*, 330−339.

(6) Galani, D.; Apenten, R. K. O. *Int. J. Food Sci. Technol.* **1999**, *34*, 467−476.

(7) Jayat, D.; Gaudin, J.-C.; Chobert, J.-M.; Burova, T. V.; Holt, C.; McNae, I.; Sawyer, L.; Haertle, T. *Biochemistry* **2004**, *43*, 6312−6321.

(8) Creamer, L. K.; Bienvenue, A.; Nilsson, H.; Paulsson, M. A.; Van Wanroij, M.; Lowe, E. K.; Anema, S.; Boland, M. J.; Jiménez-Flores, R. *J. Agric. Food Chem.* **2004**, *52*, 7660−7668.

(9) Livney, Y. D.; Verespej, E.; Dalgleish, D. G. *J. Agric. Food Chem.* **2003**, *51*, 8098−8106.

(10) Lalande, M.; Tissier, J. P.; Corrieu, G. *Biotechnol. Proc.* **1985**, *1*, 131−139.

(11) Leclerq-Perlat, M. N.; Lalande, M. *Int. Chem. Eng.* **1991**, *31*, 74−93.

(12) Xin, H.; Chen, X. D.; Özkan, N. *J. Food. Sci.* **2002**, *67*, 2702−2711.

(13) Reddy, T. T.; Lavenant, L.; Lefebvre, J.; Renard, D. *Biomacromolecules* **2006**, *7*, 323−330.

(14) Gunasekaran, S.; Xiao, L.; Ould Eleya, M. M. *J. Appl. Polym. Sci.* **2006**, *99*, 2470−2476.

(15) Xin, H.; Chen, X. D.; Özkan, N. *AIChE J.* **2004**, *50*, 1961−1973.

(16) Mercadé-Prieto, R.; Chen, X. D. *AIChE J.* **2006**, *52*, 792−803.

(17) Yamul, D. K.; Lupano, C. E. *Food Res. Int.* **2003**, *36*, 25−33.

(18) Shimada, K.; Cheftel, J. C. *J. Agric. Food Chem.* **1988**, *36*, 1018−1025.

(19) Florence, T. M. *Biochem. J.* **1980**, *189*, 507−520.

(20) Feeney, R. E.; Nashef, A. S.; Osuga, D. T.; Lee, H. S.; Ahmed, A. I.; Whitaker, J. R. *J. Agric. Food Chem.* **1977**, *25*, 245−251.

(21) Gawron, O.; Odstrchel, G. *J. Am. Chem. Soc.* **1967**, *89*, 3263−3267.

(22) Mercadé-Prieto, R.; Chen, X. D. *J. Membr. Sci.* **2005**, *254*, 157−167.

(23) Tuladhar, T. R.; Paterson, W. R.; Wilson, D. I. *Trans. 1 ChemE, Part C, Food Bioprod. Proc.* **2002**, *80*, 199−214.

(24) Bird, M. R.; Fryer, P. J. *Trans. 1 ChemE, Part C, Food Bioprod. Proc.* **1991**, *69*, 13−21.

(25) Keim, S.; Hinrichs, J. *Int. Dairy J.* **2004**, *14*, 355−363.

(26) Friedman, F. *J. Agric. Food Chem.* **1999**, *47*, 1295−1319.

(27) De Koning, P. J.; Van Rooijen, P. J. *J. Dairy Res.* **1982**, *49*, 725−736.

(28) Correia, J. J.; Lipscomb, L. D.; Lobert, S. *Arch. Biochem. Biophys.* **1983**, *300*, 105−114.

(29) Hasegawa, K.; Kitajima, S.; Takado, Y. *Agric. Biol. Chem.* **1981**, *45*, 2133−2134.

(30) Karayiannis, N. I.; MacGregor, J. T.; Bjeldanes, L. F. *Food Cosmet. Toxicol.* **1979**, *17*, 585−590.

(31) Whitaker, J. R.; Feeney, R. E. *Crit. Rev. Food Sci. Nutr.* **1983**, *19*, 173−212.

(32) Noetzold, H.; Schlegel, B.; Freimuth, U. *Z. Chem.* **1972**, *12*, 24.

(33) Cavallini, D.; Federici, G.; Barboni, E.; Marcucci, M. *FEBS Lett.* **1970**, *10*, 125−128.

(34) Florence, T. M. *J. Electroanal. Chem.* **1979**, *97*, 237−255.

(35) Xin, H.; Chen, X. D.; Özkan, N. *Trans. 1 ChemE, Part C, Food Bioprod. Proc.* **2002**, *80*, 240−246.

(36) Miller-Chou, B.; Koenig, J. L. *Prog. Polym. Sci.* **2003**, *28*, 1223−1270.

(37) Baussay, K.; Le Bon, C.; Nicolai, T.; Durand, D.; Busnel, J. P. *Int. J. Biol. Macromol.* **2004**, *34*, 21−28.

(38) Devotta, I.; Badiger, M. V.; Rajamohanan, P. R.; Ganapathy, S.; Mashelkar, R. A. *Chem. Eng. Sci.* **1995**, *50*, 2557−2569.

(39) Narasimhan, B.; Peppas, N. A. *Macromolecules* **1996**, *29*, 3283−3291.

(40) Mercadé-Prieto, R.; Chen, X. D.; Falconer, R. J.; Paterson, W. R.; Wilson, D. I. In *Proceedings of Heat Exchanger Fouling and Cleaning—Challenges and Opportunities*, Irsee, Germany, June 5−10, 2005; Müller-Steinhagen, H., Malayeri, M. R., Watkinson, P., Eds.; Engineering Conferences International: New York, 2005; http://services.bepress.com/eci/heatexchanger2005/24/.

(41) Bird, M. R. Ph.D. Thesis, University of Cambridge, United Kingdom, 1992.

(42) Zhao, Y.; Su, H.; Fang, L.; Tan, T. *Polymer* **2005**, *46*, 5368−5376.

Received for review February 27, 2006. Revised manuscript received May 19, 2006. Accepted May 31, 2006. Financial support for RM-C from the Cambridge European Trust and laboratory equipment provided by a Food Processing Faraday Fast Track award are gratefully acknowledged.

JF0605650